International Journal of Power Electronics and Drive Systems (IJPEDS)
Vol. 13, No. 4, December 2022, pp. 2244~2254
ISSN: 2088-8694, DOI: 10.11591/ijpeds.v13.i4.pp2244-2254

LCL-filter design and analysis for PWM recuperating system used in DC traction power substation

Najwatul Alisa Sabran[1], Chuen Ling Toh[1,2], Chee Wei Tan[3]
[1]Department of Electrical and Electronics Engineering, Universiti Tenaga Nasional, Selangor, Malaysia
[2]Institute of Power Engineering, Universiti Tenaga Nasional, Selangor, Malaysia
[3]School of Electrical Engineering, Universiti Teknologi Malaysia, Johor, Malaysia

Article Info

Article history:

Received Jul 15, 2022
Revised Sep 9, 2022
Accepted Sep 23, 2022

Keywords:

DC traction power substation
LCL filter
Pulse-width-modulation
Recuperating converter
Series R-damper

ABSTRACT

Voltage source inverter (VSI) had been used in dc traction power substation to deliver the trains braking energy back to the utility grid. To mitigate low order harmonics components, pulse-width-modulation (PWM) technique is commonly used in VSI controlled. As a result, the ac voltage and current waveforms may contain high frequency ripples. This paper proposes to mitigate the high frequency harmonics using LCL-filter with series *R*-damper. This filter offers good attenuation on harmonics with smaller size compare to other passive filter topologies. Theoretical analysis and simulation verification are conducted in designing the proposed filter. System level simulation had also been carried out. Sinusoidal grid current and voltage waveforms are recorded (THD<2%). This paper also includes damping losses analysis in conjunction with resonance peak suppression in designing the *R*-damper.

Corresponding Author:

Chuen Ling Toh
Department of Electrical and Electronics Engineering, Universiti Tenaga Nasional
Jalan IKRAM-UNITEN, 43000 Kajang, Selangor, Malaysia
Email: chuenling@uniten.edu.my

1. INTRODUCTION

A DC traction power substation is commonly equipped with a set of twelve-pulse rectifier transformer system [1]. As the rectifier is configured using uncontrolled power semiconductors, the braking energy harvested by metro trains have to be dissipated via resistor banks. In order to restore the braking energy back to the utility grid, voltage source inverter (VSI) is applied in the traction power substation as a recuperating converter. A VSI is connected parallel to the existing rectifier transformer system [2], [3]. It will only be triggered when a metro train is braking. The regenerative power will then be processed by the VSI and purified using a passive filter before delivering to the utility grid. These passive filters include *L*-filter [4]–[6], LC-filter [7], and LCL-filter [8]–[10] as shown in Figure 1.

L-filter is the simplest reactor design, as shown in Figure 1(a). This filter design avoids the resonance issues that occurred in the traction system. However, large inductances are demanded to limit the high switching frequency ripple. As a result, bulky and expensive *L*-filter will be integrated with an excessive voltage drop across the reactor becoming another major concern. The research in [7], an LC-filter Figure 1(b) was practically implemented in an active regeneration unit (ARU) at Rotterdam metro railway system. The LC-filter had successfully limited the propagation of high switching frequency ripple currents into the utility grid system.

Alternatively, LCL-filter has been reported to offer more accurate filtering characteristics [11]. It is proved to have better attenuation compared to *L*-filter, especially when the harmonic number is greater than 50. The total required inductances of an LCL-filter are reduced significantly compared to the conventional *L*-

filter. As a result, the volume, weight and cost of the filter are reduced. In addition, LCL-filter is also claimed to prevent inrush current. However, this filter will introduce a resonance spike at its resonant frequency. The resonance effects may trigger critical issues to the utility grid as discussed in [12], The root cause of the resonance peak is mainly due to zero impedance is measured at its resonant frequency. In order to suppress the resonance spikes, LCL-filter with damping resistance has been introduced. Figure 1 (c) shows the configuration of LCL-filter proposed in traction power substation application [8].

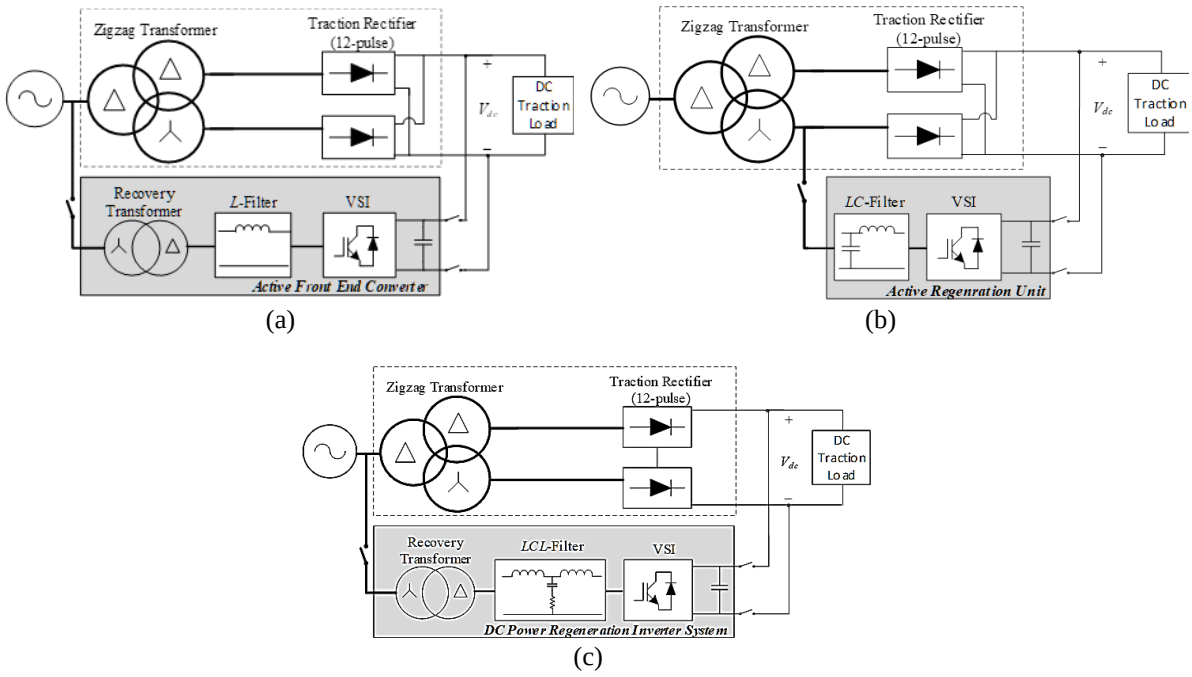

Figure 1. Different passive filters design for recuperating converter used in DC traction power substation (a) L-filter, (b) LC- filter and (c) LCL-filter

A preliminary study had been conducted via simulation to investigate the harmonic spectrum of grid current produced by a recuperating converter (VSI). In the simulation, the VSI is controlled with Pulse-Width-Modulation (PWM) scheme. The frequency modulation index, m_f, is set at 21. Thus, low order harmonics components are mitigated, and the most significant harmonics will be captured around m_f and its multiples. Table 1 tabulates the results of significant individual harmonics order of the distorted current comparing with the IEEE standard [13]. It is clearly shown that without employing any filters, most of the harmonic components exceed the current distortion limit. In order to attenuate these harmonics components, passive harmonic filters are highly demanded.

Three different topologies of passive filters shown in Figure 1 are then added in the simulation model for further study. The total reactance of three filters is set to 0.4 mH equally. Similarly, 1 mF filter capacitance are applied to LC- and LCL-filters respectively. By adding a 0.4 mH L-filter to the VSI, the harmonic orders, 19th, 23rd, 41st, and 43rd are recorded larger than the acceptance range. Therefore, the value of reactance must be increased. LC-filter shows better performance with only the 23rd order harmonic recorded at 0.7%. It is believed that by slightly increasing the filter reactance, all individual harmonic orders will comply with IEEE standard. Finally, the LCL-filter with the same set of parameters manages to attenuate all harmonics components accurately. The only drawback of LCL-filter is the damping resistor may cause some power losses in traction power substation.

Different topologies of LCL-filters had been proposed and analyzed [14]–[16]. Considering the advantages of simple design and implementation, this paper proposes LCL-filter with series R-damper for a recuperating converter used in traction power substation. An overview of the proposed LCL-filter modeling and design constraints are introduced in section 2. Section 3 shows a sample design calculation of LCL-filter parameters for a traction power substation. Section 4 presents system level simulation and verification of the proposed filter design. Finally, a short conclusion will be presented in section 5.

Table 1. Comparison of individual harmonic current distortion produced by PWM-VSI system shown in Figure 1 with IEEE Standard 519

Individual Harmonic Order, h	17	19	23	25	37	41	43	47	59	TDD_i
IEEE Standard 519 [13] (%)	1.50	1.50	0.60	0.60	0.30	0.30	0.30	0.30	0.30	5.00
VSI Without filter	0.75	13.46	12.79	0.70	1.08	5.62	5.44	0.95	3.81	21.49
VSI with L-filter	0.25	4.06	3.40	0.18	0.22	1.10	1.05	0.18	0.67	5.66
VSI with LC-filter	0.08	1.11	0.70	0.03	0.02	0.09	0.08	0.01	0.03	1.32
VSI with LCL-filter	0.08	1.07	0.60	0.03	0.01	0.06	0.05	0.01	0.02	1.24

2. LCL-FILTER MODELLING AND DESIGN CONSTRAINTS

LCL-filter is a third order filter. A three-phase equivalent circuit of the LCL-filter is shown in Figure 2(a). Each phase consists of two inductances, namely L_g and L_f, a capacitor, C_f, and a damping resistance, R_d. The parasitic resistances of inductance, L_g and L_f, are neglected in this paper.

2.1. LCL-filter modeling

The output voltages and currents produced by the converter are distorted, these electrical quantities are named as $v_{x,inv}$, and $i_{x,inv}$. The grid voltages and currents are named as v_{xg}, and i_{xg}, where x represents the phase-a, phase-b, and phase-c. Consequently, the converter voltage and current equations can be derived as:

$$v_{x,inv} = i_{x,inv}(j\omega L_f) + i_{xg}(j\omega L_g) + v_{xg} \quad (1)$$

$$i_{x,inv} = i_{xf} + i_{xg} \quad (2)$$

Since the three-phase LCL-filter can be represented as three identical single-phase systems connected in wye configuration, the filter modeling and analysis will only focus on one phase. The equivalent circuit model is shown in Figure 2(b). It is noted that the analysis on one single phase can be extrapolated to the other two phases.

Significant harmonic components always appear close to the switching frequency and its multiple of switching frequency for pulse-width-modulated VSI. These harmonic components are grouped as high frequency harmonics. Hence, the *LCL*-filter must be designed to attenuate the most significant harmonic components close to its switching frequency, for instance the 19th order harmonic shown in Table 1 (VSI without filter). Assuming that the grid voltage is pure sinusoidal which does not contain harmonics component lower than the 19th order, a simplified circuit as shown in Figure 2(c) can be applied to derive for the transfer function. The (3) expresses the transfer function from converter output voltage, $v_{x,inv}$, to grid current, i_{xg}, as [17]:

$$\frac{I_{xg}(s)}{V_{x,inv}(s)} = \frac{C_f R_d s + 1}{L_f L_g C_f s^3 + C_f R_d (L_f + L_g) s^2 + (L_f + L_g) s} \quad (3)$$

2.2. LCL-filter design constraints

The LCL-filter design is normally initiated by identifying important input variables such as the effective voltage rating and frequency of the utility grid ($v_{l\text{-}l}$, f_g), the power rating and switching frequency of the recuperating converter, (P_{inv}, f_{sw}). Hence, the base impedance, Z_B, and base capacitance, C_B, can be expressed as:

$$Z_B = \frac{(V_{l-l})^2}{P_{inv}} \quad (4)$$

$$C_B = \frac{1}{2\pi f_g Z_B} \quad (5)$$

The P_{inv} is quantified as the active power absorbed by the recuperating converter during rated operating condition. The filter capacitance, inductance and damping resistance design constraints will be further elaborated in the following sub-sections.

2.2.1. Filter capacitor, C_f

The capacitor value of the LCL-filter is normally limited to less than 5% of the rated power factor. Liserre *et al.* [18] proposed the maximum capacitance value can be estimated as follows:

$$C_{f,max} = 0.05 \cdot C_B \quad (6)$$

An analysis presented in [19] showing that the capacitance value and inductance values are inversely proportional to each other. Hence, this paper proposes to select a practical value of capacitance rated about 75% of the $C_{f,max}$.

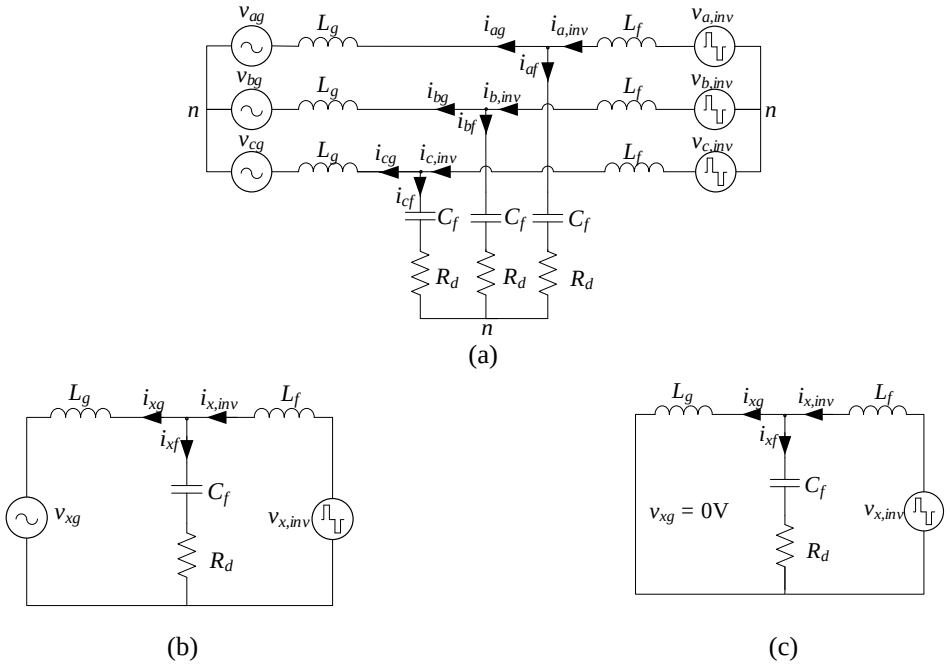

Figure 2. Equivalent circuit of (a) three-phase LCL-filter, (b) single phase LCL-filter and (c) single phase *LCL*-filter with grid voltage is assumed short-circuited

2.2.2. Converter side inductor, L_f, and grid side inductor, L_g

Two inductors namely converter side inductor, L_f, and grid side inductor, L_g, are demanded in a typical LCL-filter. In order to minimize the size and volume of the filter, L_f is normally designed in a range of 3 – 5 time larger than L_g [18].

The converter side inductor, L_f, is mainly used to limit the current ripple, $\Delta i_{x,inv}$, generated by the recuperating converter. The advantages of minimizing the ripple current, may lower the switching and conduction losses of the converter. However, this may increase the size of inductor and causing higher core losses. Hence, the acceptance range of ripple current is set to 15% – 25% of its rated current, I_{x,inv_rated}. In (7) shows the definition of I_{x,inv_rated}:

$$I_{x,inv\_rated} = \frac{\sqrt{2}P_{inv}}{\sqrt{3}V_{l-l}} \quad (7)$$

The minimum inductance value of L_f, can then be formulated as follows with the assumption that the maximum ripple current occurred at 50 % duty cycle [20].

$$L_{f,min} = \frac{V_{dc}}{4\Delta i_{x,inv} f_{sw}} \quad (8)$$

Where V_{dc} represent the dc link voltage supply to the recuperating converter. While the grid side inductor, L_g, is commonly designed by multiplying the converter side inductor value with a factor of r,

$$L_g = rL_f \quad (9)$$

The relationship of current ripple attenuation from $i_{x,inv}$ to i_g versus the factor of r had been discussed in [18], [21]. The larger the factor of r will improve the quality of the grid current; however, the cost and size of the filter will also increase.

2.2.3. Damping resistor, R_d

The damping resistor, R_d, is designed to ensure the system stability and suppress the resonance peak of the LCL-filter. A typical damping resistance value is generally estimated as 33.33% of the filter capacitive reactance at resonance frequency [22].

$$R_d = \frac{1}{3} X_{C_{(fres)}} = \frac{1}{3}\left(\frac{1}{2\pi f_{res} C_f}\right) \tag{10}$$

The power losses of a properly damped LCL-filter can be estimated as:

$$P_d = 3R_d \cdot \sum_h \left[i_{xf}(h)\right]^2 \tag{11}$$

The main current harmonics order, $i_{xf}(h)$, used in (11) are the significant harmonics component appeared near to the switching frequency and its multiples.

2.3. Resonance frequency, f_{res}

By neglecting the effect of the damping resistance, R_d, in the transfer function from converter output voltage, $v_{x,inv}$, to grid current, i_{xg}, the resonance frequency, f_{res}, of the LCL-filter can be formulated as [23], [24]:

$$f_{res} = \frac{1}{2\pi}\sqrt{\frac{(L_f + L_g)}{L_f L_g C_f}} \tag{12}$$

The practical range of resonance frequency is normally limited by the utility grid frequency, f_g, and the PWM switching frequency of the recuperating converter, f_{sw}. The range is proposed to set as follows [18]:

$$10 f_g < f_{res} < \frac{1}{2} f_{sw} \tag{13}$$

For instance, the LCL-filter shown in Figure 1 (c) is connected to a 50 Hz utility grid system. Assume that the filter parameters are chosen with the resonance frequency is estimated at 581 Hz. In this design, the VSI must be operated with switching frequency set higher than 1162 Hz. This is to effectively attenuate the significant group of harmonics appear around the switching frequency. Without choosing an appropriate switching frequency may cause the VSI operate improperly and further amplify the significant group of harmonics.

The variation of LCL-filter parameters mainly changes the resonant frequency. Figure 3 (a) shows a Bode plot diagrams of the transfer function, (3) of an LCL-filters with different sets of LCL parameters. By increasing the value of the inductances and capacitance of the filters, the resonant frequency will be shifted towards a lower frequency range. On the other hand, the resonant spikes can be suppressed by increasing the value of damping resistance as shown in Figure 3 (b).

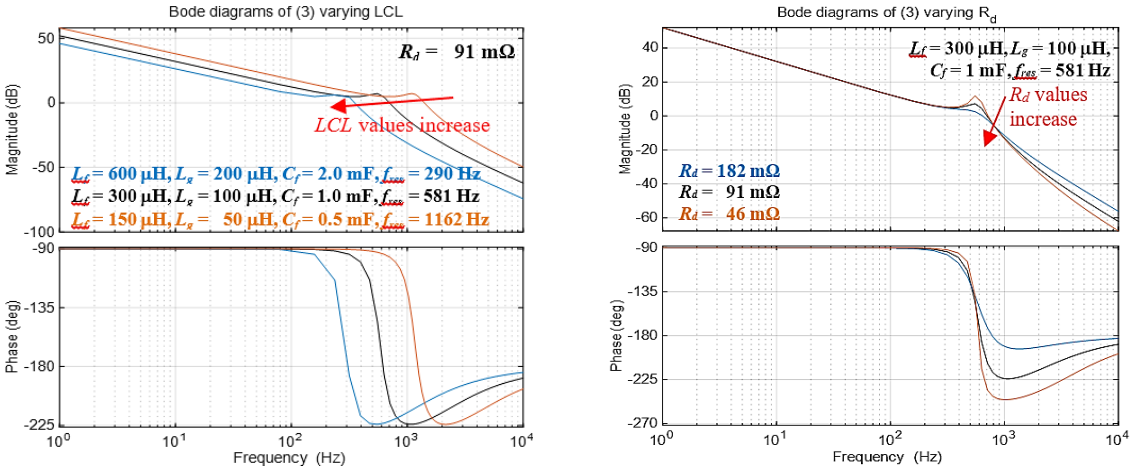

Figure 3. Bode plot of the transfer function from converter output voltage, $v_{x,inv}$, to grid current, i_{xg}, (a) variation of LCL parameters with fixed R_d and (b) variation of R_d with identical LCL parameters (f_{res} = 581 Hz)

3. *LCL*-FILTER DESIGN FOR RECUPERATING CONVERTER

This paper adopts the LCL-filter design procedure presented in [18] and [22]. The recuperating converter is assumed to be configured in an existing dc traction power substation as shown in Figure 1 (c). Table 2 summarizes the system parameters used to initiate the LCL-filter design [25]. Table 3 listed all the numerical value of LCL-filter design categorized into theoretical value and practical value. Theoretical values are obtained by directly applying in (4)-(10), whereas the practical values are finalized with considering the available off-the-shelf component with proper examination of resonance frequency constraints.

Firstly, the base impedance, Z_B, and base capacitance, C_B, can be calculated using (4) and (5), as 114 mΩ, and 27.90 mF. Thus, the maximum filter capacitance can be determined as 1.395 mF. A practical value of 1mF filter capacitance is selected. Next, the rated current of the VSI is computed with (7) as 4.19 kA. The current ripple is proposed to set at 15% of its rated current which resulting to estimate the minimum inductance requirement on the converter side with approximate 265 μH. This paper proposes to select a larger L_f, rated at 300 μH to determine an applicable grid-side inductors. The r factor is suggested to varies from 0.2 until 1.0 to properly attenuate the grid current ripple. As a result, L_g values varying from 60 μH until 300 μH is applicable. Three random values of L_g (60μH, 100μH, and 300 μH) are selected for resonance frequency evaluation using Bode plot shown in Figure 4 (a). The results shown that only 100 μH grid side inductance fulfill the resonance frequency constraint in the dc traction substation. Equation (13) can be further derived with the system parameters given in Table 2, which yields the practical range of resonance frequency as 500 Hz < f_{res} < 675 Hz.

Lastly, a typical damping resistor value is estimated as 0.091 Ω. Figure 4 (b) illustrates the effect of varying the value of damping resistance will result in different level of resonance peak suppression. This paper chooses 0.10 Ω damping resistor as an initiate value as it offers the lowest peak resonance. However, a larger value of resistance may cause more power losses and degrade the system efficiency. Further evaluation will be conducted via system level simulation in the next section.

Table 2. Parameters of the traction substation system integrating with a recuperating converter (VSI)

Parameters	Value	Parameters	Value
Grid voltage, v_{grid}	33 kV	VSI rated power, P_{inv}	3 MW
Grid frequency, f_g	50 Hz	VSI dc-link voltage, V_{dc}	900 V
Recovery Transformer voltage rating, *HV/LV*	33/0.585 kV	VSI PWM switching frequency, f_{sw}	1350 Hz

Table 3. Proposed *LCL*-filter parameters

Equation	Theoretical Parameters	Value	Finalized practical Parameters	Value
(6)	Maximum filter capacitor, $C_{f,max}$	1.395 mF	Filter capacitor, C_f,	1 mF
(8)	Minimum converter side inductor, $L_{f,min}$	265.182 μH	Converter side inductor, L_f	300 μH
(9)	Applicable range of grid side inductor L_g	60 μH < L_g < 300 μH	Grid side inductor, L_g	100 μH
(10)	Minimum damping resistor, $R_{d,min}$	0.91 Ω	Damping resistor, R_d	0.10 Ω

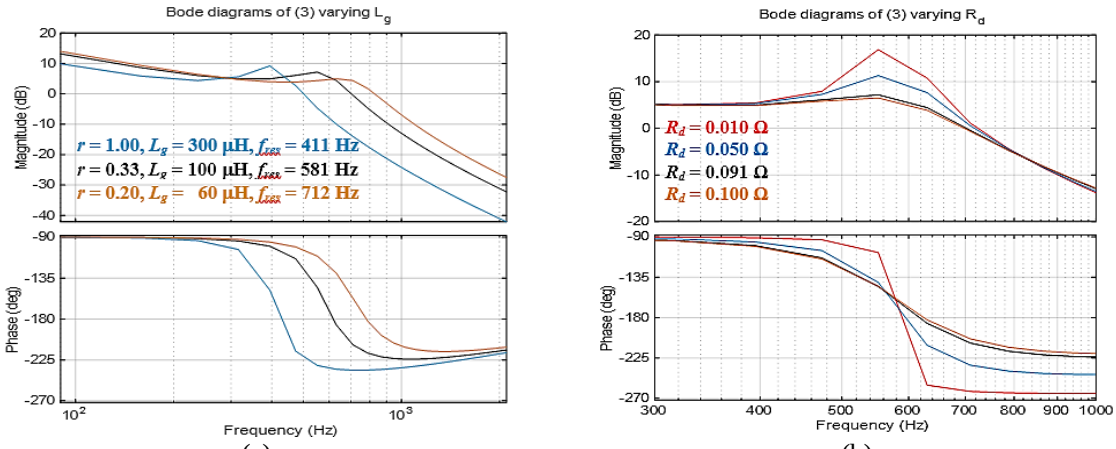

(a) (b)

Figure 4. Bode plot of the transfer function from converter output voltage, $v_{x,inv}$, to grid current, i_{xg}, (a) variation of L_g with other parameters fixed at C_f = 1 mF, L_f = 300 μH, and R_d = 91 mΩ and (b) variation of R_d with other parameters fixed at C_f = 1 mF, L_f = 300 μH, and L_g = 100 μH

4. SYSTEM LEVEL SIMULATION AND ANALYSIS

In order to analyze the effectiveness of the proposed *LCL*-filter, a simulation model as shown in Figure 5 (a) is developed using MATLAB/Simulink. The utility grid, the twelve-pulse rectifier transformer system, and the recovery transformer shown in Figure 1(c) are modelled as *RL*-source load. The ac-source is modelled with the recovery transformer low-voltage rating, i.e. 585 V, 50 Hz. Referring to field data given in [26], the dc link voltage is rated at 900 V when a train is braking. The recuperating system will be activated during this occurrence. The voltage source inveter (VSI) circuit is presented in Figure 5 (b), this VSI is modulated with sinusoidal pulse-width-modulation (SPWM) technique. The fundamantal of SPWM technique had been presented in [27], [28]. Pure sinusoidal ac voltages, v_g, are assumed as the voltage references in this simulation. As shown in Figure 5 (c), three-phase *vg_ref* signals are first being normalized to ease the application of the amplitude modulation index, m_a. The modulating waves are then being compared with carrier wave to generate respective gate signals to control the IGBT switches of the VSI. Table 4 summarizes all the simulation parameters.

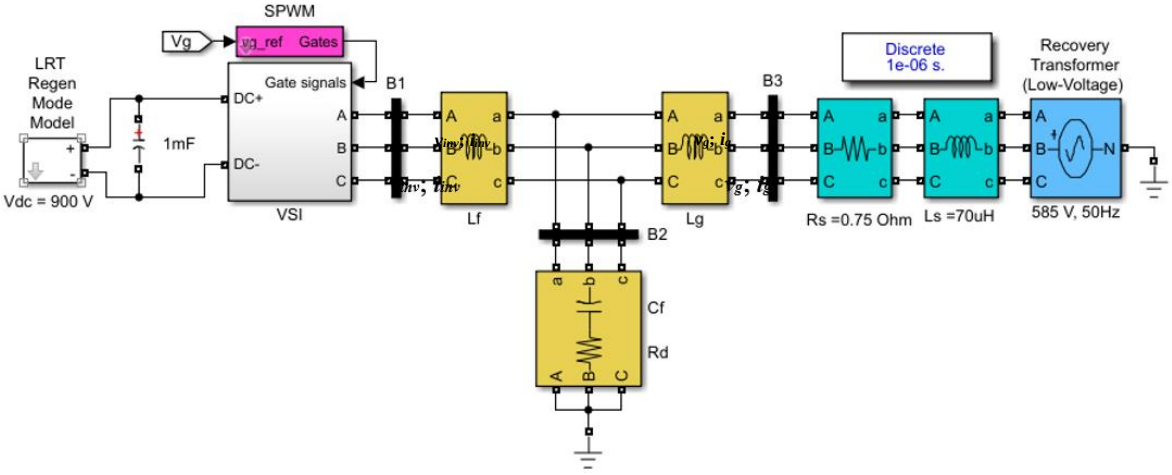

(a)

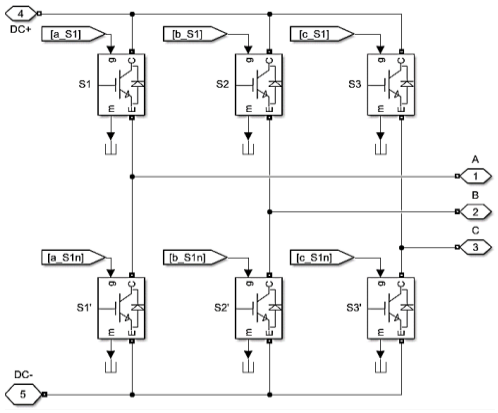

(b)

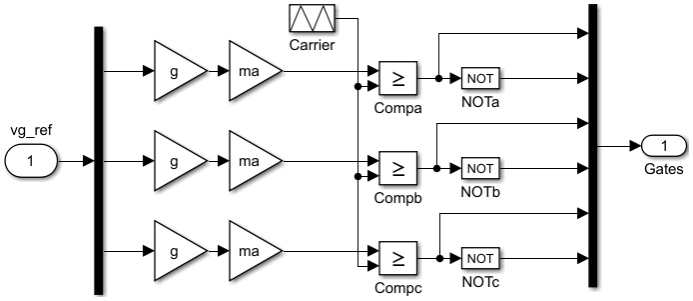

(c)

Figure 5. Simulation model of (a) recuperating converter system, (b) VSI, and (c) SPWM

Table 4. Simulation parameters

Voltage source inverter		*LCL*-filter		DC traction substation (load)	
DC-link Voltage, $V_{dc,}$	900 V	$C_{f,}$	1 mF	Resistive-Load, R_{load}	0.75 Ω
DC-link capacitor, $C_{dc,}$	1 mF	L_f	300 µH	Inductive-Load, L_{load}	70 µH
PWM switching frequency, f_{sw}	1350 Hz	L_g	100 µH	AC Souce-Load, $v_{ac,l\text{-}l}$	585 V
Amplitude modulation index, m_a	1	R_d	0.10 Ω	AC Souce-Load frequency, f_{ac}	50 Hz

Figure 6 presents the phase voltages waveform produced by the VSI before and after passing through the LCL-filter. The phase voltages, $v_{x,inv}$, shown in Figure 6(a) are badly distorted due to the high switching events. The simulator recorded the total voltage distortion as 68.75%. The harmonic spectrum shown in Figure 7(a) shows that significant harmonics are recorded around m_f (27th order) and its multiples. The most significant pair of individual voltage harmonics (25th and 29th orders) are noted at about 31% of its fundamental voltage. With the integration of the proposed LCL-filter, sinusoidal voltage waveforms are captured in Figure 6(b). The total voltage harmonic distortion recorded in Figure 7(b) is less than 2%.

The inverter currents, $i_{x,inv}$, consist of high ripples with $\Delta i_{x,inv}$, measured about 300 A is presented in Figure 8(a). The total current harmonics distortion is simulated as 7.11 % with individual current harmonics percentage tabulated in Table 5. Current harmonics of $i_{x,inv}$, in the order of 25th, 29th, 53rd and 55th are found exceeding the limit set by IEEE Standard 519. Hence, the system requires passive filter for harmonics attenuation. In term of current harmonic distortion, the proposed LCL-filter (with r = 0.333), is capable to limit all significant harmononic components within the permitted range set by [13]. As a result, good quality of grid current waveforms are observed in Figure 8(b).

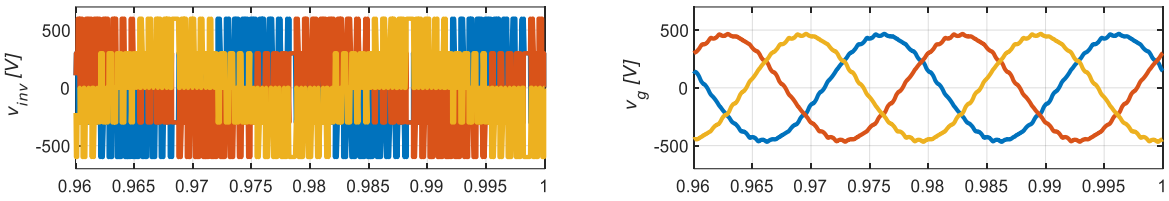

Figure 6. Simulation results of voltage waveforms measured at (a) converter side (before filtering) and (b) grid-side (after filtering)

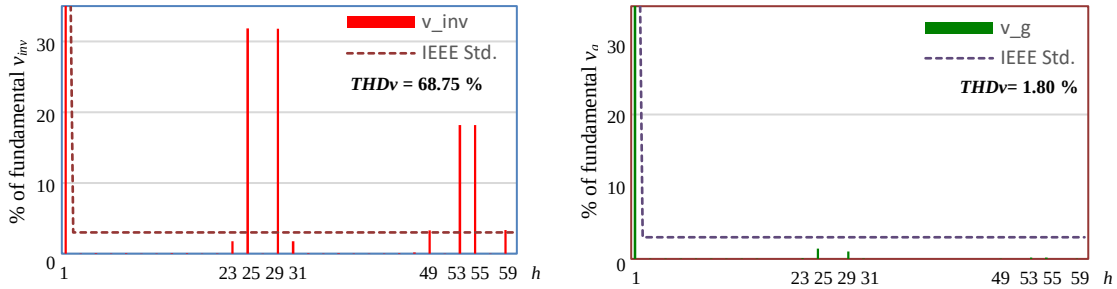

Figure 7. Harmonic spectrum of phase voltages shown in Figure 6

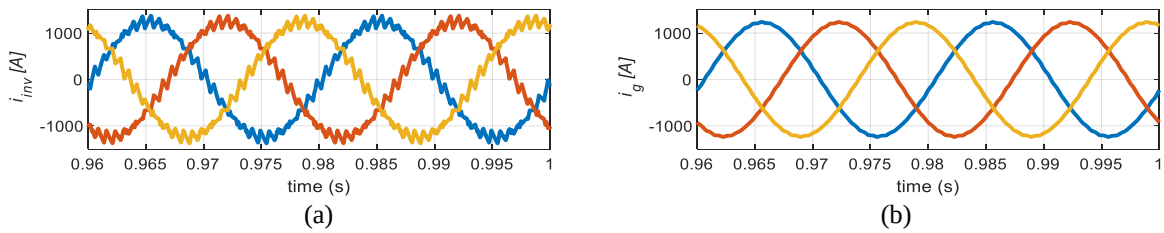

Figure 8. Simulation results of current waveforms measured at (a) converter side (before filtering) and (b) grid-side (after filtering)

Further analysis on grid current harmonic attenuation is carried out by varying the r factor. The recuperating converter system is simulated with two different r factors conforms with the practical range of resonance frequency (500 Hz < f_{res} < 675 Hz). The simulation results proved that further increasing the grid-side inductor, L_g, (with r = 0.50), may further attenuate each of the current harmonic components. However, reducing of L_g (with r = 0.25), may result in improper attenuation of the 25th order harmonic current as shown in Table 5.

Table 5. Comparison of individual harmonic current distortion percentage of $i_{x,inv}$, and $i_{x,g}$ with IEEE standard 519. (LCL-filter parameters: C_f = 1 mF, L_f = 300 µH, and R_d = 100 mΩ)

Individual Harmonic Order, h	23	25	29	31	49	53	55	59	TDD_i
IEEE Standard 519 [13] (%)	0.60	0.60	0.60	0.60	0.30	0.30	0.30	0.30	5.00
$i_{x,inv}$ (%)	0.31	5.10	4.34	0.22	0.26	1.32	1.27	0.22	7.11
$i_{x,g}$ (%) with r = 0.25, f_{res} = 650 Hz	0.04	0.63	0.44	0.02	0.01	0.06	0.06	0.01	0.78
$i_{x,g}$ (%) with r = 0.33, f_{res} = 581 Hz	0.04	0.57	0.39	0.02	0.01	0.05	0.05	0.01	0.70
$i_{x,g}$ (%) with r = 0.50, f_{res} = 503 Hz	0.03	0.47	0.32	0.01	0.01	0.04	0.04	0.01	0.57

Lastly, three damping resistances with the values of 0.10 Ω, 0.05 Ω, and 0.01 Ω are applied in the simulation model to estimate the potential power losses caused by damping resistor. Figure 9 shows the simulation results of the harmonics currents, $i_{x,f}$, The proposed filter is designed successfully with high frequency current ripples being drained out via the filter capatiors, C_f. These harmonic currents will also pass through the damping resistor, R_d. In general, varying the values of damping resistors will not diminish the filtering effects as all the harmonics currents looks identical in Figure 9 (a), Figure 9 (b), and Figure 9 (c). However, the simulation results shown that the damping loss is proportional to damping resistance in Figure 10.

As shown in Figure 10 (a), a 0.10 Ω damping resistance may consume an average of 4.13 kW power. Although the 0.10 Ω damping resistor offers excellent supression on the resonant peak as shown in Figure 4 (b), this paper proposes to redesign the damping resistor for the *LCL*-filter in order to minimize the damping losses. In Figure 10 (b) and Figure 10 (c), the damping losses are predicted to be reduced significantly by selecting a smaller value of damping resistors. For instance, a 0.05 Ω damping resistor will introduce about 2 kW losses while 0.01 Ω damping resistor will minimize the losses to 400 W. To sum up, the damping resistor is finalized with the value of 0.05 Ω with the consideration on providing good suppression of the peak resonance as well as introducing acceptable power losses for the recuperating system.

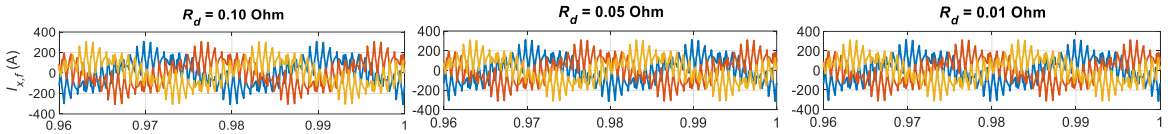

(a) (b) (c)

Figure 9. Three-phase harmonic currents flow through the damping resistor, R_d, rated at (a) 0.10 Ω, (b) 0.05 Ω, and (c) 0.01 Ω

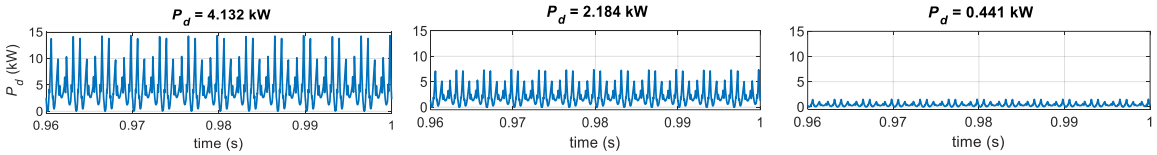

(a) (b) (c)

Figure 10. Instantaneous power consumed by the damping resistor, R_d, rated at (a) 0.10 Ω, (b) 0.05 Ω, and (c) 0.01 Ω

5. CONCLUSION

Voltage source inverter (VSI) is commonly used in dc traction power substation to restore the trains braking energy back to the utility grid. This inverter introduces high switching ripples to the grid voltage and current waveforms. Therefore, this paper proposes to implement an LCL-filter with series *R*-damper to

mitigate the high frequency harmonics. A comparison study of *L*-, LC-, and LCL-filters in attenuating individual harmonics components had been carried out. It is proven that LCL-filter may offer better harmonic attenuation with significant size reduction. The LCL-filter is designed by examining the filter resonance frequency, which must lie in between the grid frequency and the converter switching frequency. A system level simulation study had been carried out to validate the feasibility of the proposed filter. The simulation results proved that sinusoidal grid voltage and current with less than 2 % harmonic distortion are obtained. The grid-side inductor can be designed with *r* factor set at 0.333. The *R*-damper will not diminish the filtering effects of an LCL-filter. This paper proposes to design the damping resistance as about 20% of the filter capacitive reactance at resonance frequency.

ACKNOWLEDGEMENTS

The authors are pleased to express their appreciation to the Universiti Tenaga Nasional for sponsoring the BOLD Refresh 2025 to conduct this research.

REFERENCES

[1] S. A. Assefa, A. B. Kebede, and D. Legese, "Harmonic analysis of traction power supply system: case study of Addis Ababa light rail transit," *IET Electrical Systems in Transportation*, vol. 11, no. 4, pp. 391-404, 2021, doi: 10.1049/els2.12019.

[2] G. Zhang, Z. Tian, P. Tricoli, S. Hillmansen, Y. Wang and Z. Liu, "Inverter operating characteristics optimization for DC traction power supply systems," *IEEE Transactions on Vehicular Technology*, vol. 68, no. 4, pp. 3400-3410, 2019, doi: 10.1109/TVT.2019.2899165.

[3] A. Jitpaiboon, T. Kulworawanichpong and T. Ratniyomchai, "Energy saving of a DC railway system by applying inverting substations," in *International Conference on Power, Energy and Innovations (ICPEI)*, 2021, pp. 85-88, doi: 10.1109/ICPEI52436.2021.9690646.

[4] W. A. G. de Jager, "Buddy bidirectional supply for traction substations," in *European Conference on Power Electronics and Applications*, 2011, pp. 1-10.

[5] I. Madariaga *et. al.*, "Device and control procedure for recovery of kinetic energy in railway systems," USA Patent US8146513B2, 2009.

[6] C. H. Bae, M. S. Han, Y. K. Kim, C. Y. Choi and S. J. Jang, "Simulation study of regenerative inverter for DC traction substation," *International Conference on Electrical Machines and Systems*, 2005, pp. 1452-1456, doi: 10.1109/ICEMS.2005.202789.

[7] W. A. G. de Jager, M. Huizer and E. K. H. van der Pols, "Implementation of an active regeneration unit in a traction substation," *European Conference on Power Electronics and Applications*, 2014, pp. 1-9, doi: 10.1109/EPE.2014.6911054.

[8] S.-J. Jang, C.-Y. Choi, C.-H. Bae, S.-H. Song and C.-Y. Won, "Study of regeneration power control inverter for DC traction with active power filter ability," in *Conference of IEEE Industrial Electronics Society*, 2005. IECON 2005., 2005, pp. 6 pp.-, doi: 10.1109/IECON.2005.1569088.

[9] M. Popescu, A. Bitoleanu and M. Dobriceanu, "Investigations on the coupling LCL filter in active traction substations," in *International Conference on Optimization of Electrical and Electronic Equipment (OPTIM) & Intl Aegean Conference on Electrical Machines and Power Electronics (ACEMP)*, 2017, pp. 654-659, doi: 10.1109/OPTIM.2017.7975043.

[10] M. Popescu, A. Bitoleanu and A. Preda, "A new design method of an LCL filter applied in active DC-traction substations," *IEEE Transactions on Industry Applications*, vol. 54, no. 4, pp. 3497-3507, 2018, doi: 10.1109/TIA.2018.2819968.

[11] H. R. Karshenas and H. Saghafi, "Performance investigation of LCL filters in grid connected converters," *IEEE/PES Transmission & Distribution Conference and Exposition: Latin America*, 2006, pp. 1-6, doi: 10.1109/TDCLA.2006.311646.

[12] R. Antar, M. Y. Suliman, and A. A. Saleh, "Harmonics resonance elimination technique using active static compensation circuit," *Bulletin of Electrical Engineering and Informatics*, vol. 10, no. 5, pp. 2405-2413, 2021, doi: 10.11591/eei.v10i5.3148.

[13] IEEE Recommended Practice and Requirements for Harmonic Control in Electric Power Systems, IEEE, pp. 6–7, 2014, doi: 10.1109/IEEESTD.2014.6826459.

[14] R. N. Beres, X. Wang, M. Liserre, F. Blaabjerg and C. L. Bak, "A review of passive power filters for three-phase grid-connected voltage-source converters," *IEEE Journal of Emerging and Selected Topics in Power Electronics*, vol. 4, no. 1, pp. 54-69, March 2016, doi: 10.1109/JESTPE.2015.2507203.

[15] F. Zhong, G. W. Chang and K. T. Nguyen, "A new damping scheme of llcl filter for grid-tied pv inverter output harmonics mitigation," in *International Conference on Harmonics & Quality of Power (ICHQP)*, 2022, pp. 1-6, doi: 10.1109/ICHQP53011.2022.9808771.

[16] M. Jayaraman and VT Sreedevi, "Power quality improvement in a cascadedmultilevel inverter interfaced grid connected system using a modified inductive-capacitive-inductive filter with reduced power loss and improved harmonic attenuation," *Energies*, vol. 10, no. 1834, pp. 1–23, 2017, doi: 10.3390/en10111834.

[17] A. Milicua, G. Abad, "Control of grid-conncted converters," *Power Electronics and Electric Drives for Traction Applications*, Wiley, pp. 148–221, 2017, doi: 10.1002/9781118954454.ch4.

[18] M. Liserre, F. Blaabjerg and S. Hansen, "Design and control of an LCL-filter-based three-phase active rectifier," in IEEE *Transactions on Industry Applications*, vol. 41, no. 5, pp. 1281-1291, Sept.-Oct. 2005, doi: 10.1109/TIA.2005.853373.

[19] R. N. Beres, X. Wang, M. Liserre, F. Blaabjerg and C. L. Bak, "A review of passive power filters for three-phase grid-connected voltage-source converters," *IEEE Journal of Emerging and Selected Topics in Power Electronics*, vol. 4, no. 1, pp. 54-69, March 2016, doi: 10.1109/JESTPE.2015.2507203.

[20] T. Lahlou, M. Abdelrahem, S. Valdes and H. -G. Herzog, "Filter design for grid-connected multilevel CHB inverter for battery energy storage systems," in *International Symposium on Power Electronics, Electrical Drives, Automation and Motion (SPEEDAM)*, 2016, pp. 831-836, doi: 10.1109/SPEEDAM.2016.7525972.

[21] M. Chapparband, D. K. Sameeksha and M. Miranda, "Analysis of LCL filter design for grid tied power converter and its effect on THD," *International Conference on Signal Processing and Integrated Networks (SPIN)*, 2020, pp. 850-855, doi: 10.1109/SPIN48934.2020.9070927.

[22] M. F. Yaakub, M. A. M. Radzi, M. Azri, F. H. M. Noh, "LCL filter design for grid-connected single-phase flyback microinverter: a step by step guide," *International Journal of Power Electronics and Drive Systems (IJPEDS)*, vol. 12, no. 3, pp. 1632–1643, 2021, doi: 10.11591/ijpeds.v12.i3.pp1632-1643.
[23] Q. Liu, L. Peng, Y. Kang, S. Tang, D. Wu and Y. Qi, "A novel design and optimization method of an *LCL* filter for a shunt active power filter," in *IEEE Transactions on Industrial Electronics*, vol. 61, no. 8, pp. 4000-4010, 2014, doi: 10.1109/TIE.2013.2282592.
[24] L. Zhou, Z. Liu, Y. Ji, D. Ma, J. Wang and L. Li, "A improved parameter design method of LCL APF interface filter," *IEEE International Conference on Artificial Intelligence and Computer Applications (ICAICA)*, 2020, pp. 948-952, doi: 10.1109/ICAICA50127.2020.9182457.
[25] C. L. Toh, P. C. Ooi, "Design a nine-level modular multilevel converter for DC railway electrification system," *International journal of power electronics and drive system (IJPEDS)*, vol. 11, no. 1, pp. 151–159, 2020, doi: 10.11591/ijpeds.v11.i1.pp151–159.
[26] M. Rajaratnam, P. Guyard, N. Mazet, "Plan of instruction-traction power sub-station (TPSS) overall system description," Konsortium CMC-COLAS-UNIWAY, Kuala Lumpur, 2016.
[27] H. Attia, H. S. Che, T. K. S. Freddy, A. Elkhateb, "Bipolar and unipolar schemes for confined band variable switching frequency PWM based inverter," *International Journal of Electrical and Computer Engineering (IJECE)*, vol. 11, no. 5, pp. 3763–3771, 2021, doi: 10.11591/ijece.v11i5.pp3763-3771.
[28] B. Addo-Yeboa and G. Owusu, "Modification of SPWM -based controller for voltage source inverter," *International Conference on Electronics, Computers and Artificial Intelligence (ECAI)*, 2022, pp. 1-5, doi: 10.1109/ECAI54874.2022.9847430.

BIOGRAPHIES OF AUTHORS

Najwatul Alisa Sabran received the B. Eng. Degree in electrical power engineering from Universiti Tenaga Nasional (UNITEN), Kajang, Malaysia, in 2021. She is an electrical engineer with Tenaga Nasional Berhad (TNB), Malaysia. Her research interests include power electronics converter design and mitigation of power quality issues. She can be contacted at email: ep0102731@student.uniten.edu.my.

Chuen Ling Toh received the B. Eng. and M. Eng. degree in electrical engineering, both from Universiti Teknologi Malaysia (UTM), Skudai, Malaysia, in 2002 and 2005 respectively; and her Ph.D in Electrical Power Engineering from Norwegian University of Science and Technology (NTNU), Trondheim, Norway, in 2014. Currently, she is a Senior Lecturer at the Universiti Tenaga Nasional, Kajang, Malaysia. Her teaching and research interests include the field of power electronics, motor drive systems and field programmable gate array applications. She is also an engineer registered with Board of Engineers Malaysia and a professional technologist registered with Malaysia Board of Technologists. She can be contacted at email: chuenling@uniten.edu.my.

Chee Wei Tan received his B.Eng. degree in Electrical Engineering (First Class Honors) from Universiti Teknologi Malaysia (UTM), in 2003 and a Ph.D. degree in Electrical Engineering from Imperial College London, London, U.K., in 2008. He is currently an associate professor at Universiti Teknologi Malaysia and a member of the Power Electronics and Drives Research Group, School of Electrical Engineering, Faculty of Engineering. His research interests include the application of power electronics in renewable/alternative energy systems, control of power electronics and energy management system in microgrids. He is also a Chartered Engineer registered with Engineering Council, UK, a professional engineer registered with Board of Engineers Malaysia and a professional technologist registered with Malaysia Board of Technologists. He is actively participating in IEEE activities and conferences, which he is also the chair of the IEEE Power Electronic Society (PELS) Malaysia Chapter for year 2018. He was awarded the Malaysia Research Star Award (High Impact Paper – Engineering and Technologies) 2018 by the Ministry of Education Malaysia. He can be contacted at email: cheewei@utm.my.